

# FLC tuned with Gravitational Search Algorithm for Nonlinear Pose Filter

Trenton S. Sieb, Ajay Singh, Lorelei Guidos, and Hashim A. Hashim  
Software Engineering

Department of Engineering and Applied Science

Thompson Rivers University, Kamloops, British Columbia, Canada, V2C-0C8  
siebt19@mytru.ca, ludhera17@mytru.ca, guidosl16@mytru.ca, and hhashim@tru.ca

**Abstract**—Nonlinear pose (*i.e.*, attitude and position) filters are characterized with simpler structure and better tracking performance in comparison with other methods of pose estimation. A critical factor when designing a nonlinear pose filter is the selection of the error function. Conventional design of nonlinear pose filter design trade-off between fast adaptation and robustness. This paper introduces a new practical approach based on fuzzy rules for on-line continuous tuning of the nonlinear pose filter. Each of input and output membership functions are optimally tuned using graphical search algorithm optimization considering both pose error and its rate of change. The proposed approach is characterized with high adaptation features and strong level of robustness. Therefore, the proposed approach results of robust and fast convergence properties. The simulation results show the effectiveness of the proposed approach considering uncertain measurements and large error in initialization.

## I. INTRODUCTION

FROM space craft and satellites to vehicles underwater and in the air, knowing an accurate three-dimensional estimate of the pose of a rigid-body is a task that is vitally important [1–4]. The pose consists of two components: 1) orientation and 2) position. Attitude is often used in place of orientation so they will be used interchangeably. Attitude reconstruction is often done using an algebraic approach. This involves using an algorithm such as QUEST [5] or singular value decomposition (SVD) [6] that takes two or more noncollinear inertial frame vectors as well as the object’s body frame vectors. However, this method is quite susceptible to noise and bias which can damage results and make them unusable. This effect is particularly potent if the rigid-body is equipped with a low cost IMU.

An alternative method that has been used historically to address the issue of estimating the attitude is a Gaussian or nonlinear deterministic filter. The Kalman filter (KF), extended KF (EKF), and multiplicative EKF (MEKF) are all examples within the family of Gaussian filters that consider the unit quaternion to represent attitude [3,4]. However, the attitude problem being of a nonlinear nature, gives nonlinear deterministic attitude filters evolved on the Special Orthogonal Group  $SO(3)$ , an acute advantage over Gaussian filters. They outperform in many aspects such as with simpler derivation

and representation, reduced processing power, and improved tracking convergence [3,7,8].

In order to ensure accurate position estimation, a good attitude estimation is required. Furthermore, as with attitude, it is better to use a nonlinear approach, using filters evolved on the Special Euclidean Group  $SE(3)$  [9–12]. These filters require measurements that can be derived from a group velocity vector, on-board vectorial measurements from a device such as an IMU, landmark measurements from a builtin vision system, and an estimate of the bias in the measured velocity [9,10,12]. Nonlinear filters are commonly used along with a computer vision system with a monocular camera and an IMU. In [11], the pose filter was developed on  $SE(3)$  with a proven exponentially stable performance. Although the implementation of said filter requires pose reconstruction, modifications can be made that allow function using purely a set of vectorial measurements [13,14], which adds simplicity and avoids the reconstruction. However, despite the simplicity in [11,13,14], the results of data collected show that these filters are highly sensitive to noise in the measurements. Additionally, the conventional design of pose filters [13,14] is characterized with slow convergence of tracking error.

Fuzzy logic controller (FLC) is an intelligent approach which showed essential solutions in several control applications, for example,  $\mathcal{L}_1$  adaptive controller tuned with FLC [15], adaptive fuzzy controller for mobile robots [16], and others. Also, evolutionary techniques went through accelerated developments over the last few decades. They have the capability to be an optimal fit with a wide range of control applications such as the gravitational search algorithm (GSA) which was proposed as a global search technique in [17]. The necessity to tune originally fixed coefficients of controllers and filters has been widely used in various applications, such as [15,18]. Moreover, they have fundamental role in data mining [19–21].

Thereby, this study presents fuzzy tuning the gain of the nonlinear pose filter where the fuzzy input and output membership functions are optimized using GSA, considering the pose error and its rate of change. The FLC-based tuning is an on-line carried out during the estimation process. GSA determines the optimal values of input and output membership functions through off-line tuning. FLC is introduced to enhance the trade-off between robustness and fast convergence. The gain of the nonlinear pose filter is dynamically tuned, hence resulting in better performance. Actually, the proposed technique

solves the dilemma of fast adaptation and fast convergence response. The proposed method is simpler and can be easily implemented.

The rest of the paper is organized as follows: Section II presents a short overview of numerical and mathematical representations of  $SO(3)$  and  $SE(3)$  parameterization. Section III articulates the pose problem, demonstrates the filter structure and error criteria, and presents the nonlinear structure of the attitude filter. Section IV presents the proposed filter strategy, which includes a brief introduction of the gravitational search algorithm, fuzzy logic controller and a diagram of the implementation process. Section V shows the obtained results and validates the robustness of the proposed filters. Finally, Section VI completes the work with concluding comments.

## II. PRELIMINARIES OF $SE(3)$

In this paper  $\{\mathcal{B}\}$  denotes body-frame of a reference and  $\{\mathcal{I}\}$  denotes the inertial-frame of a reference.  $\|x\| = \sqrt{x^\top x}$  denotes Euclidean norm for all  $x \in \mathbb{R}^p$ .  $\mathbf{I}_p$  denotes a  $p$ -by- $p$  identity matrix.  $R \in \{\mathcal{B}\}$  denotes an orientation of a rigid-body in the space which is commonly termed attitude. Define  $SO(3)$  as the Special Orthogonal Group

$$SO(3) = \{R \in \mathbb{R}^{3 \times 3} \mid RR^\top = R^\top R = \mathbf{I}_3, \det(R) = +1\}$$

with  $\mathbf{I}_3$  being a 3-by-3 identity matrix and  $\det(\cdot)$  is a determinant. Let  $SE(3)$  be the Special Euclidean Group where

$$SE(3) = \{H \in \mathbb{R}^{4 \times 4} \mid R \in SO(3), P \in \mathbb{R}^3\}$$

Also,  $H \in SE(3)$  is commonly known as the homogeneous transformation matrix that expresses the pose of the rigid-body as below

$$H = \begin{bmatrix} R & P \\ 0_{1 \times 3} & 1 \end{bmatrix} \in SE(3) \quad (1)$$

where  $P$  and  $R$  are position and attitude, respectively, and  $0_{1 \times 3}$  being a zero row. The Lie-algebra related to  $SO(3)$  is defined as  $\mathfrak{so}(3)$  and is given by

$$\mathfrak{so}(3) = \{X \in \mathbb{R}^{3 \times 3} \mid X^\top = -X\}$$

where  $X$  is a skew symmetric matrix. Consider the map  $[\cdot]_\times : \mathbb{R}^3 \rightarrow \mathfrak{so}(3)$  to be

$$[x]_\times = \begin{bmatrix} 0 & -x_3 & x_2 \\ x_3 & 0 & -x_1 \\ -x_2 & x_1 & 0 \end{bmatrix} \in \mathfrak{so}(3), \quad x = \begin{bmatrix} x_1 \\ x_2 \\ x_3 \end{bmatrix}$$

For any  $\mathcal{Y} = [y_1^\top, y_2^\top]^\top$  with  $y_1, y_2 \in \mathbb{R}^3$ , one has

$$[\mathcal{Y}]_\wedge = \begin{bmatrix} [y_1]_\times & y_2 \\ 0_{1 \times 3} & 0 \end{bmatrix} \in \mathfrak{se}(3)$$

$\mathfrak{se}(3)$  is the Lie algebra of  $SE(3)$  given by

$$\mathfrak{se}(3) = \left\{ [\mathcal{Y}]_\wedge \in \mathbb{R}^{4 \times 4} \mid \exists y_1, y_2 \in \mathbb{R}^3 : [\mathcal{Y}]_\wedge = \begin{bmatrix} [y_1]_\times & y_2 \\ 0_{1 \times 3} & 0 \end{bmatrix} \right\}$$

Also, for  $x, y \in \mathbb{R}^3$  and  $x_0, y_0 \in \mathbb{R}$  consider the following definition

$$\begin{bmatrix} x \\ x_0 \end{bmatrix} \wedge \begin{bmatrix} y \\ y_0 \end{bmatrix} = \begin{bmatrix} x \times y \\ x_0 y - y_0 x \end{bmatrix} \in \mathbb{R}^6$$

For more details on  $SO(3)$  visit [3,4] and  $SE(3)$  visit [9,10].

## III. PROBLEM FORMULATION

This section aims to present the pose problem, pose measurements, error criteria and nonlinear pose filter design.

### A. Pose Dynamics and Measurements

As mentioned earlier, pose of a rigid-body in the space consists of two components: orientation (attitude) and position. Attitude is given by  $R \in SO(3)$  while position is defined as  $P \in \mathbb{R}^3$ . Note that  $R \in \{\mathcal{B}\}$  and  $P \in \{\mathcal{I}\}$ . The pose filtering problem is depicted in Fig. 1

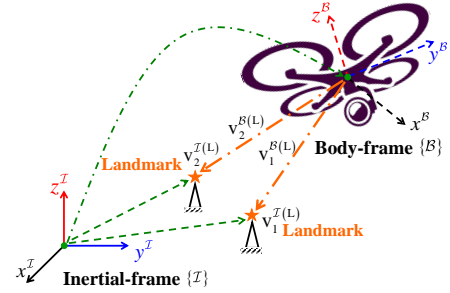


Fig. 1. Pose filtering problem of a rigid-body [10,22].

Let the superscripts  $\mathcal{B}$  and  $\mathcal{I}$  be elements related to  $\{\mathcal{B}\}$  and  $\{\mathcal{I}\}$ , respectively. Attitude can be represented, given  $n$  observations in the inertial-frame and their measurements in the body-frame, where the  $i$ th body-frame vector measurement is defined by

$$v_i^{\mathcal{B}} = R^\top v_i^{\mathcal{I}} + b_i^{\mathcal{B}} + n_i^{\mathcal{B}} \in \mathbb{R}^3 \quad (2)$$

where  $v_i^{\mathcal{I}}$  is a known observation,  $b_i^{\mathcal{B}}$  is unknown bias, and  $n_i^{\mathcal{B}}$  is unknown noise for all  $i = 1, 2, \dots, n$ . The equivalent normalization of  $v_i^{\mathcal{I}}$  and  $v_i^{\mathcal{B}}$  in Eq. (2) is expressed as

$$v_i^{\mathcal{I}} = \frac{v_i^{\mathcal{I}}}{\|v_i^{\mathcal{I}}\|}, \quad v_i^{\mathcal{B}} = \frac{v_i^{\mathcal{B}}}{\|v_i^{\mathcal{B}}\|} \quad (3)$$

The position of a moving vehicle can be reestablished for a known  $R$  and  $L$  known landmarks. The  $i$ th landmark measurement in the body-frame can be expressed as [9,10]

$$y_i^{\mathcal{B}} = R^\top (p_i^{\mathcal{I}} - P) + \bar{b}_i^{\mathcal{B}} + \bar{n}_i^{\mathcal{B}} \in \mathbb{R}^3 \quad (4)$$

with  $p_i^{\mathcal{I}}$  being a known landmark,  $\bar{b}_i^{\mathcal{B}}$  being unknown bias, and  $\bar{n}_i^{\mathcal{B}}$  being unknown noise for all  $i = 1, 2, \dots, L$ .

**Assumption 1.** (Pose observability) The pose of a rigid body is observable if one of the following three cases is met

**case 1.** At least two non-collinear vectors in Eq. (3) and one landmark in Eq. (4) are available.

**case 2.** At least one non-collinear vectors in Eq. (3) and two landmark in Eq. (4) are available.

**case 3.** At least three landmarks in Eq. (4) are available.

The dynamics of the homogeneous transformation matrix in Eq. (1) is given by

$$\dot{H} = H [\mathcal{Y}]_\wedge \quad (5)$$

such that  $\dot{R} = R [\Omega]_\times$ ,  $\dot{P} = RV$ ,  $\mathcal{Y} = [\Omega^\top, V^\top]^\top \in \mathbb{R}^6$  denotes a group velocity vector. Also,  $\Omega \in \mathbb{R}^3$  is the true

angular and  $V \in \mathbb{R}^3$  is the translational velocity. Unfortunately, the measured velocity vector is corrupted by uncertain components

$$\mathcal{Y}_m = \mathcal{Y} + b + \omega \in \{\mathcal{B}\} \quad (6)$$

where  $\mathcal{Y}_m = [\Omega_m^\top, V_m^\top]^\top$ ,  $b = [b_\Omega^\top, b_V^\top]^\top$ , and  $\omega = [\omega_\Omega^\top, \omega_V^\top]^\top$  such that  $b_\Omega, b_V \in \mathbb{R}^3$  are the unknown constant bias and  $\omega_\Omega, \omega_V \in \mathbb{R}^3$  are unknown noise. Let the estimate of  $\mathbf{H}$  in Eq. (1) be

$$\hat{\mathbf{H}} = \begin{bmatrix} \hat{R} & \hat{P} \\ 0_{1 \times 3} & 1 \end{bmatrix} \quad (7)$$

where  $\hat{R}$  and  $\hat{P}$  are the estimates of  $R$  and  $P$ , respectively. Let the error between  $\mathbf{H}$  and  $\hat{\mathbf{H}}$  be

$$\tilde{\mathbf{H}} = \hat{\mathbf{H}}\mathbf{H}^{-1} = \begin{bmatrix} \tilde{R} & \tilde{P} \\ 0_{1 \times 3} & 1 \end{bmatrix} \quad (8)$$

with  $\tilde{R} = \hat{R}R^\top$  and  $\tilde{P} = \hat{P} - \tilde{R}P$  being errors in attitude and position, respectively. This work aims to drive  $\tilde{\mathbf{H}} \rightarrow \mathbf{H}$  with fast adaptation and high measures of robustness to ensure that  $\tilde{P} \rightarrow 0_{3 \times 1}$ ,  $\tilde{R} \rightarrow \mathbf{I}_3$ , and  $\tilde{\mathbf{H}} \rightarrow \mathbf{I}_4$ .

### B. Nonlinear Pose Filter Design

The filter design in this Section follows the structure in [14] where the contribution is the introduction of adaptively tuned gain. Consider the following filter design [14]

$$\begin{aligned} & \begin{bmatrix} x \\ x_0 \end{bmatrix} \wedge \begin{bmatrix} y \\ y_0 \end{bmatrix} = \begin{bmatrix} x \times y \\ x_0 y - y_0 x \end{bmatrix} \in \mathbb{R}^6, x, y \in \mathbb{R}^3 \\ \mathbf{U} &= \frac{1}{2} \sum_{i=1}^{N_L} s_i^L \hat{\mathbf{T}} \begin{bmatrix} y_i^B \\ 1 \end{bmatrix} \wedge \begin{bmatrix} p_i^T \\ 1 \end{bmatrix} \\ & + \frac{1}{2} \sum_{i=1}^{N_R} s_i^R \hat{\mathbf{T}} \begin{bmatrix} v_i^B \\ 0 \end{bmatrix} \wedge \begin{bmatrix} v_i^T \\ 0 \end{bmatrix} \\ \dot{\hat{\mathbf{T}}} &= \hat{\mathbf{T}} [\mathcal{Y}_m - \hat{b} + \mathbf{K}W] \wedge \\ \dot{\hat{b}} &= -\gamma \begin{bmatrix} \hat{R}^\top & 0_{3 \times 3} \\ -\hat{R}^\top [\hat{P}] & \hat{R}^\top \end{bmatrix} \mathbf{U} \\ W &= \begin{bmatrix} \hat{R} & 0 \\ [\hat{P}]_\times & \hat{R} \end{bmatrix}^\top \mathbf{U} \end{aligned} \quad (9)$$

with  $\mathbf{K} = 1 + k_{\text{op}} \in \mathbb{R}_+$ ,  $k_{\text{op}}$  being a nonnegative constant to be designed in the following Section,  $\gamma$  being a positive constant, and  $\hat{b}$  being the estimates of  $b$ .

**Remark 1.** [8,10] *The classic design of nonlinear filters on SE(3) [14] select the gain  $\mathbf{K}$  to be a positive constant. The weakness of such an approach is that smaller values of  $\mathbf{K}$  lead to slower transient performance with high measures of robustness in the steady-state (less oscillatory performance). In contrast, greater values of  $\mathbf{K}$  results of the faster transient performance with less robustness measures in the steady-state (higher oscillation).*

Consistent with Remark 1, the aim is to tune  $\mathbf{K}$  to be large at a large error and small at a small error which could lead to 1) fast convergence capabilities, and 2) high measures of robustness.

## IV. PROPOSED APPROACH

In consistence with Remark 1,  $\mathbf{K}$  must be set large enough at large values of error and small enough at small values of error. Hence, fuzzy logic controller (FLC) will be utilized to tune  $\mathbf{K}$  in accordance with the error in pose. The basic structure of FLC is composed of 1) fuzzification, which includes the input membership function, 2) rule base, and 3) defuzzification, which includes the output membership function. Aiming to achieve robust and fast adaptation, the parameters of input and output membership functions of the FLC will be selected using the gravitational search algorithm (GSA) algorithm.

### A. Gravitational Search Algorithm

GSA is an analytical technique, first introduced in 2009 based on Newton's laws of universal gravitation [17]. The algorithm is aligned to the inductive reasoning of gravitational law: "for any two objects, every object is attracted to the other object by a force which is directly proportional to their mass and inversely proportional to their square distance". Based on gravity principle, the gravitational force among any two nodes is

$$F(t) = G(t) \frac{M_1 M_2}{D(t)^2} \quad (10)$$

with  $M_1$  and  $M_2$  being masses of node 1 and 2, respectively,  $D = \|X_j, X_k\|^2 + \delta$  denoting the Euclidean distance between two nodes  $i$  and  $k$ , and  $\delta$  denoting a small positive constant.  $G$  is a gravitational constant and at time  $t$  is given by

$$G(t) = G(t_0) \exp(-\alpha t / T_{\text{final}}) \quad (11)$$

where  $G(t_0)$  denotes the gravitational constant at  $t_0$ ,  $\alpha$  denotes a positive constant, and  $T_{\text{final}}$  denotes final search time. Actually,  $T_{\text{final}}$  represents the total number of iterations in the search. The gravitational constant at time  $t$  and the initial masses have a major role in the cost function value. Heavier mass indicates a better node. Similarly, lighter mass refers to a worse node. Define a new variable relative to the  $j$ th node

$$m_j(t) = \frac{\mathcal{C}_j(t) - \mathcal{C}_j^{\text{worse}}(t)}{\mathcal{C}_j^{\text{best}}(t) - \mathcal{C}_j^{\text{worse}}(t)} \quad (12)$$

with  $N$  being total number of nodes  $\forall j = 1, 2, \dots, N$ ,  $\mathcal{C}_j(t)$  being the  $j$ th cost function at iteration  $t$ ,  $\mathcal{C}_j^{\text{worse}}(t)$  being the worst cost function (highest value), and  $\mathcal{C}_j^{\text{best}}(t)$  being the best cost function (smallest value) in the search process. Accordingly, the total mass of the  $j$ th node is given by

$$\bar{M}_j(t) = \frac{m_j(t)}{\sum_{j=1}^N m_j(t)} \quad (13)$$

The acceleration of the node is defined as below

$$a_{j,k}(t) = \frac{F_{j,k}(t)}{\bar{M}_j(t)} \quad (14)$$

for all  $j = 1, 2, \dots, N$  and  $k = 1, 2, \dots, P$  such that  $N$  denotes the total number of nodes and  $P$  denotes the total number of parameters within a single node to be optimized. Also,  $F_{j,k}(t)$  denotes the force of a particle at position  $x_{j,k}(t)$  and  $\bar{M}_j(t)$  is the mass of the  $j$ th particle. The velocity

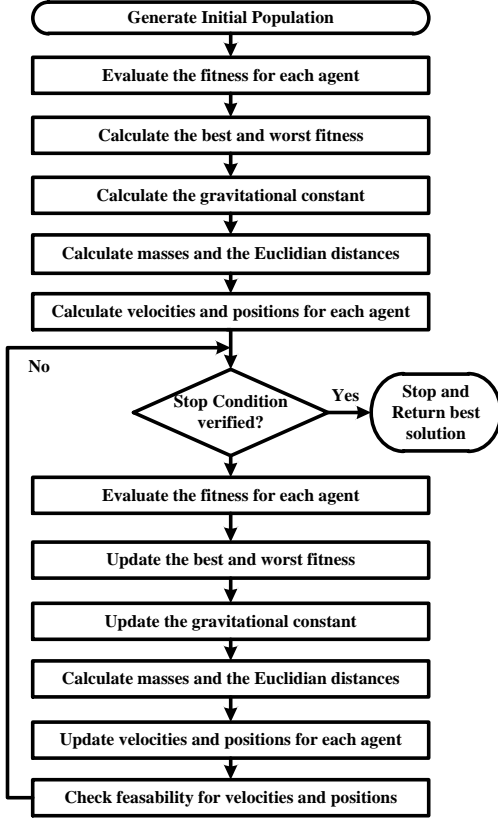


Fig. 2. Graphical illustration of GSA algorithm

associated with parameter  $k$  in node  $j$  at iteration  $t + 1$  is defined by

$$\vartheta_{j,k}(t+1) = \text{rand}_j \vartheta_{j,k}(t) + a_{j,k}(t) \quad (15)$$

with  $\text{rand}_j$  being a random number between 0 and 1. Finally, the position of parameter  $k$  in node  $j$  at iteration  $t+1$  is given by

$$x_{j,k}(t+1) = x_{j,k}(t) + \vartheta_{j,k}(t+1) \quad (16)$$

It is worth mentioning that a small set  $K_{\text{best}}$  is used to contain the best solution over the whole search process. At the end of every iteration, the small set  $K_{\text{best}}$  is updated. The complete flow chart of GSA is illustrated in Fig. 2.

### B. Pose Filter: GSA and Optimal Fuzzy-tuning

FLC is a well-known approach that is widely used in various control applications. In this work, FLC is employed to control the nonlinear pose filter through fine tuning the feedback filter gain. The tuning of the filter would contribute to solving the bottleneck between fast convergence of pose error and robustness.

The main objective of this work is constructing input and output membership functions for FLC that are able to reduce the pose error. This would be achieved through the iterative process. The membership functions are set to be triangular for both fuzzy inputs and outputs. Each membership function has five linguistic variables, namely, very large ( $VL$ ), large ( $L$ ),

TABLE I  
RULE BASE OF FLC.

$\Delta e \setminus e$	$VL$	$L$	$M$	$S$	$VS$
$VL$	$VL$	$VL$	$VL$	$V$	$V$
$V$	$VL$	$VL$	$VL$	$V$	$M$
$M$	$VL$	$VL$	$V$	$M$	$M$
$S$	$VL$	$VL$	$M$	$M$	$S$
$VS$	$VL$	$VL$	$M$	$S$	$VS$

medium ( $M$ ), small ( $S$ ) and very small ( $VS$ ). Thus, the setting parameters of the input and output membership function are selected through the optimization process. The optimization of input and output membership functions values is done using GSA in Subsection IV-A. See the rule base of the proposed filter in Table I. The  $j$ th cost function is selected as below

$$\begin{aligned} C_j &= 0.3 \times e_{tr} + e_{ss} \\ e_{tr} &= \sum_{0 \leq t \leq 1} \|\tilde{R}\|_I + 0.2 \times \sum_{0 \leq t \leq 1} \|\tilde{P}(t)\| \\ e_{ss} &= \sum_{4 \leq t \leq 14} \|\tilde{R}\|_I + 0.2 \times \sum_{4 \leq t \leq 14} \|\tilde{P}(t)\| \end{aligned} \quad (17)$$

with  $e_{tr}$  being the transient time over the period of 0 to 1 seconds,  $e_{ss}$  being the steady-state error over the period of 4 to 15 seconds for a sampling time of 0.01 seconds. 0.3 and 0.2 in Eq. (17) are weighting factors and are selected after a set of trials. The input and output membership functions have constraint values given in Eq. (18) and Eq. (19), respectively

$$\begin{cases} [0, 0, 0] & \leq [0, 0, k_1] \leq [0, 0, 0.15] \\ [0, 0, 0.1] & \leq [k_2, k_3, k_4] \leq [0.2, 0.2, 0.2] \\ [0.05, 0.1, 0.1] & \leq [k_5, k_6, k_7] \leq [0.2, 0.3, 0.4] \\ [0.1, 0.2, 0.3] & \leq [k_8, k_9, k_{10}] \leq [0.4, 0.8, 0.8] \\ [0.2, 1, 1] & \leq [k_{11}, 1, 1] \leq [0.7, 1, 1] \end{cases} \quad (18)$$

$$\begin{cases} [0, 0, 0] & \leq [0, 0, k_{12}] \leq [0, 0, 10] \\ [0, 0, 5] & \leq [k_{13}, k_{14}, k_{15}] \leq [10, 20, 30] \\ [5, 10, 20] & \leq [k_{16}, k_{17}, k_{18}] \leq [20, 50, 50] \\ [20, 20, 40] & \leq [k_{19}, k_{20}, k_{21}] \leq [50, 70, 90] \\ [30, 100, 100] & \leq [k_{22}, 100, 100] \leq [70, 100, 100] \end{cases} \quad (19)$$

where  $k_1$  to  $k_{22}$  are parameters of the membership functions to be optimized using GSA with respect to the cost function defined in Eq. (17) in addition to the constraints in Eq. (18) and Eq. (19). Fig. 3 illustrates the complete diagram of the proposed filter strategy.

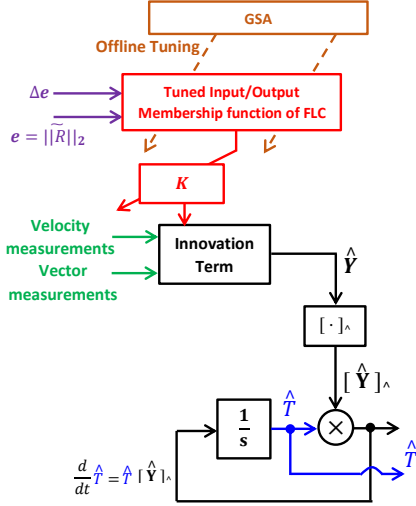


Fig. 3. Proposed filter diagram

## V. SIMULATION

### A. Pose Measurements and Initialization

Consider the following set of measurements

$$\begin{cases} \Omega_m = \Omega + b_\Omega + n_\Omega \text{ (rad/sec)} \\ V_m = V + b_V + n_V \text{ (m/sec)} \\ \Omega = [\sin(0.7t), 0.7 \sin(0.5t + \pi), 0.5 \sin(0.3t + \frac{\pi}{3})]^\top \\ V = 0.3 [\sin(0.6t), \sin(0.4t), \sin(0.1t)]^\top \\ b_\Omega = 0.1 [1, -1, 1]^\top, \quad n_\Omega = \mathcal{N}(0, 0.2) \\ b_V = 0.1 [2, 5, 1]^\top, \quad n_V = \mathcal{N}(0, 0.1) \\ v_i^B = R^\top v_i^T + b_i^B + n_i^B, \quad v_3^B = v_1^B \times v_2^B \\ v_1^T = \frac{1}{\sqrt{3}} [1, -1, 1]^\top, \quad v_2^T = [0, 0, 1]^\top \\ b_1^B = 0.1 [1, -1, 1]^\top, \quad n_1^B = \mathcal{N}(0, 0.1) \\ b_2^B = 0.1 [0, 0, 1]^\top, \quad n_2^B = \mathcal{N}(0, 0.1) \\ y_1^B = R^\top (p_1^T - P) + \bar{b}_1^B + \bar{n}_1^B \\ p_1^T = [0.5, \sqrt{2}, 1]^\top, \quad \bar{n}_1^B = \mathcal{N}(0, 0.1) \end{cases}$$

where  $n = \mathcal{N}(0, 0.1)$  is a random noise vector with 0 mean and standard deviation of 0.1. Also, for very large error, consider the following:

$$T(0) = \mathbf{I}_4, \quad \hat{T}(0) = \begin{bmatrix} -0.829 & 0.293 & 0.343 & 4 \\ 0.399 & 0.157 & 0.903 & -3 \\ 0.210 & 0.943 & -0.257 & 5 \\ 0 & 0 & 0 & 1 \end{bmatrix}$$

### B. GSA Implementation

For the implementation, Eq. (16) represents the position of the particle and Eq. (12) denotes mass with respect to the quality of the cost function.  $N$  is the number of nodes in the space. The total number of iterations is 250. The number of nodes to be allocated is  $N = 100$ . Within every node, there are 22 parameters to be optimized,  $k_1$  to  $k_{22}$ , given in Eq. (18) and (19). Fig. 4 and 5 represent the optimized input and output membership function after completing the search process.

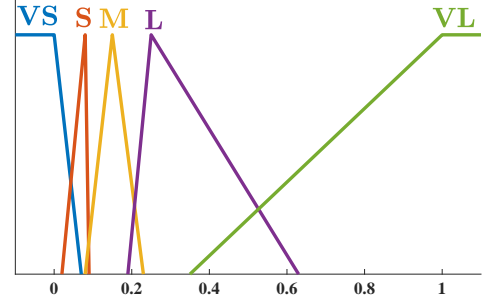


Fig. 4. Error and rate of error membership functions

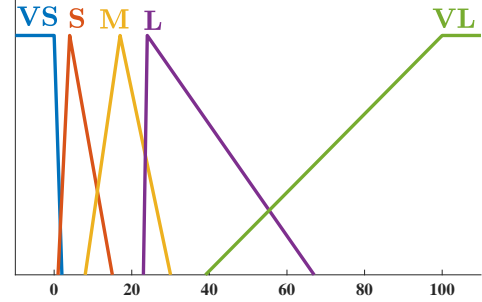
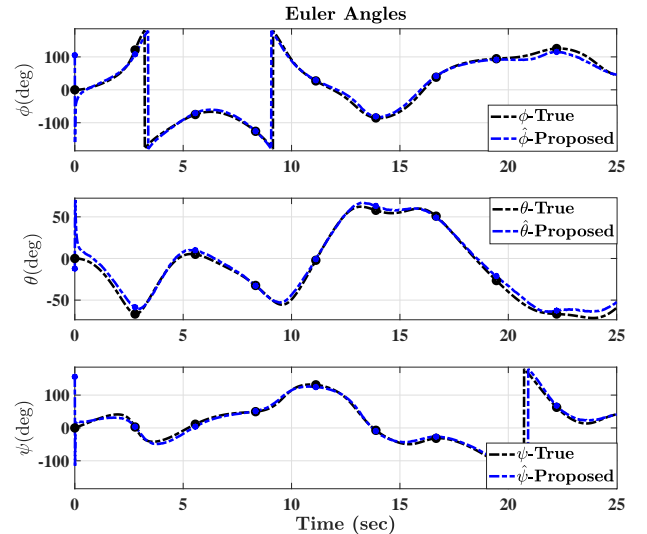


Fig. 5. Output membership function

### C. Robustness of the Proposed Approach

Fig. 6 and 7 reveal smooth and fast tracking convergence of estimated Euler angles versus the true Euler angles ( $\phi, \theta, \psi$ ) and estimated position versus the true position, respectively. The proposed approach shows impressive tracking performance against uncertain measurements and large error in initialization. This can be confirmed by the results presented in Fig. 8 that show how the filter initiated at large values of error and converged very close to the origin in a short time. As such, Fig. 8 reveals that the proposed approach is characterized with fast adaptation and robustness.

Fig. 6. Euler angles ( $\phi, \theta, \psi$ ): True vs Estimate (Proposed)

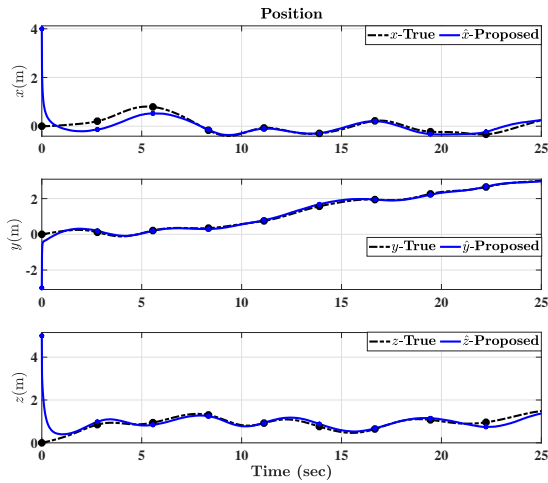


Fig. 7. Position ( $x, y, z$ ): True vs Estimate (Proposed)

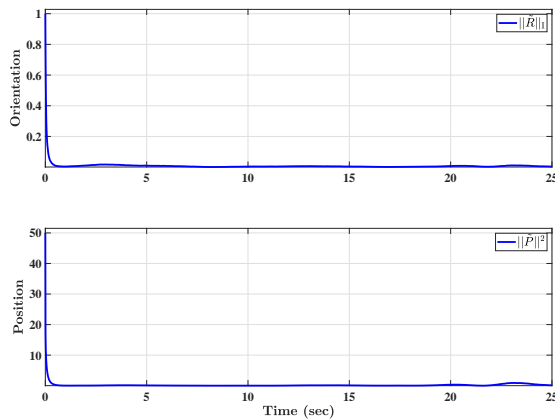


Fig. 8. Normalized Error: Position & Euclidean distance

## VI. CONCLUSION

This paper presents the fuzzy logic controller (FLC) design, tuned with the gravitational search algorithm (GSA) for a nonlinear pose filter. GSA optimization has been utilized to find the optimal parameters of the input and output membership functions of the FLC. The proposed approach tunes the adaptation gain on-line, to allow for fast adaptation. In addition, owing to the smooth tuning, the proposed filter maintains a high measure of robustness. Simulation results illustrate fast convergence of the pose (attitude and position) error and robustness against large initialization error and uncertain measurements. In the future, there is a plan to implement the proposed approach on a real module and compare it against existing algorithms in the literature. Also, we are planning to compare GSA against other methods of evolutionary techniques.

## ACKNOWLEDGMENT

The authors would like to thank **Maria Shaposhnikova** for proofreading the article.

## REFERENCES

[1] H. A. Hashim, "Guaranteed performance nonlinear observer for simultaneous localization and mapping," *IEEE Control Systems Letters*, vol. 5, no. 1, pp. 91–96, 2021.

[2] F. L. Markley, "Attitude error representations for kalman filtering," *Journal of guidance, control, and dynamics*, vol. 26, no. 2, pp. 311–317, 2003.

[3] H. A. Hashim, L. J. Brown, and K. McIsaac, "Nonlinear stochastic attitude filters on the special orthogonal group 3: Ito and stratonovich," *IEEE Transactions on Systems, Man, and Cybernetics: Systems*, vol. 49, no. 9, pp. 1853–1865, 2019.

[4] H. A. Hashim, "Systematic convergence of nonlinear stochastic estimators on the special orthogonal group  $SO(3)$ ," *International Journal of Robust and Nonlinear Control*, vol. 30, no. 10, pp. 3848–3870, 2020.

[5] M. D. Shuster and S. D. Oh, "Three-axis attitude determination from vector observations," *Journal of Guidance, Control, and Dynamics*, vol. 4, pp. 70–77, 1981.

[6] F. L. Markley, "Attitude determination using vector observations and the singular value decomposition," *Journal of the Astronautical Sciences*, vol. 36, no. 3, pp. 245–258, 1988.

[7] R. Mahony, T. Hamel, and J.-M. Pfimlin, "Nonlinear complementary filters on the special orthogonal group," *IEEE Transactions on Automatic Control*, vol. 53, no. 5, pp. 1203–1218, 2008.

[8] H. A. H. Mohamed, "Nonlinear attitude and pose filters with superior convergence properties," *Ph. D. Western University*, 2019.

[9] H. A. Hashim and F. L. Lewis, "Nonlinear stochastic estimators on the special euclidean group  $SE(3)$  using uncertain imu and vision measurements," *IEEE Transactions on Systems, Man, and Cybernetics: Systems*, vol. PP, no. PP, pp. 1–14, 2020.

[10] H. A. Hashim, L. J. Brown, and K. McIsaac, "Nonlinear pose filters on the special euclidean group  $SE(3)$  with guaranteed transient and steady-state performance," *IEEE Transactions on Systems, Man, and Cybernetics: Systems*, pp. 1–14, 2019.

[11] G. Baldwin, R. Mahony, J. Trunpf, T. Hamel, and T. Chevignon, "Complementary filter design on the special euclidean group  $se(3)$ ," in *Control Conference (ECC), 2007 European*. IEEE, 2007, pp. 3763–3770.

[12] H. A. Hashim, L. J. Brown, and K. McIsaac, "Nonlinear stochastic position and attitude filter on the special euclidean group 3," *Journal of the Franklin Institute*, vol. 356, no. 7, pp. 4144–4173, 2019.

[13] G. Baldwin, R. Mahony, and J. Trunpf, "A nonlinear observer for 6 dof pose estimation from inertial and bearing measurements," in *Robotics and Automation, 2009. ICRA'09. IEEE International Conference on*. IEEE, 2009, pp. 2237–2242.

[14] M.-D. Hua, T. Hamel, R. Mahony, and J. Trunpf, "Gradient-like observer design on the special euclidean group  $se(3)$  with system outputs on the real projective space," in *Decision and Control (CDC), 2015 IEEE 54th Annual Conference on*. IEEE, 2015, pp. 2139–2145.

[15] H. A. Hashim, S. El-Ferik, and M. A. Abido, "A fuzzy logic feedback filter design tuned with pso for L1 adaptive controller," *Expert Systems with Applications*, vol. 42, no. 23, pp. 9077–9085, 2015.

[16] H. Shi, M. Xu, and K.-S. Hwang, "A fuzzy adaptive approach to decoupled visual servoing for a wheeled mobile robot," *IEEE Transactions on Fuzzy Systems*, 2019.

[17] E. Rashedi, H. Nezamabadi-Pour, and S. Saryazdi, "Gsa: a gravitational search algorithm," *Information sciences*, vol. 179, no. 13, pp. 2232–2248, 2009.

[18] Y. Yu, Z. Yang, C. Han, and H. Liu, "Fuzzy adaptive back-stepping sliding mode controller for high-precision deflection control of the magnetically suspended momentum wheel," *IEEE Transactions on Industrial Electronics*, vol. 65, no. 4, pp. 3530–3538, 2017.

[19] A. E. Eltoukhy, Z. Wang, F. T. Chan, and X. Fu, "Data analytics in managing aircraft routing and maintenance staffing with price competition by a stackelberg-nash game model," *Transportation Research Part E: Logistics and Transportation Review*, vol. 122, pp. 143–168, 2019.

[20] A. E. Eltoukhy, Z. Wang, F. T. Chan, and S. H. Chung, "Joint optimization using a leader-follower stackelberg game for coordinated configuration of stochastic operational aircraft maintenance routing and maintenance staffing," *Computers & Industrial Engineering*, vol. 125, pp. 46–68, 2018.

[21] A. E. Eltoukhy, Z. Wang, F. T. Chan, S. Chung, H.-L. Ma, and X. Wang, "Robust aircraft maintenance routing problem using a turnaround time reduction approach," *IEEE Transactions on Systems, Man, and Cybernetics: Systems*, 2019.

[22] H. A. Hashim, L. J. Brown, and K. McIsaac, "Guaranteed performance of nonlinear pose filter on  $SE(3)$ ," in *Proceedings of the American Control Conference (ACC)*, 2019, pp. 1–6.